In Vivo Biomechanical Assessment of a Novel Handle-Based Wheelchair Drive

Markus Puchinger, Pia Stefanek, Karin Gstaltner, Marcus G. Pandy, and Margit Gföhler

***Abstract*— Push-rim wheelchair propulsion frequently causes severe upper limb injuries in people relying on the wheelchair for ambulation. To address this problem, we developed a novel handle-based wheelchair propulsion method that follows a cyclic motion within ergonomic joint ranges of motion. The aim of this study was to measure hand propulsion forces, joint excursions and net joint torques for this novel propulsion device and to compare its performance against traditional push-rim wheelchair propulsion. We hypothesized that under similar conditions, joint excursions of this novel handle-based device will remain within their ergonomic range and that the effectiveness of the propulsion forces will be higher, leading to lower average propulsion forces compared to push-rim propulsion and reducing the risk of injury. Eight paraplegic subjects propelled the new device at two different loads on a custom-made wheelchair-based test rig. Video motion capture and force sensors were used to monitor shoulder and wrist joint kinematics and kinetics. Shoulder and wrist loads were calculated using a modified upper-extremity Wheelchair Propulsion Model available in OpenSim. The results show that with this novel propulsion device joint excursions are within their recommended ergonomic ranges, resulting in a reduced range of motion of up to 30% at the shoulder and up to 80% at the wrist, while average resultant peak forces were reduced by up to 20% compared to push-rim propulsion. Furthermore, the lower net torques at both the shoulder and wrist demonstrate the potential of this novel propulsion system to reduce the risk of upper-extremity injuries.**

***Index Terms*— Ergonomics, handle, propulsion, shoulder, upper-limb, wheelchair, wrist.**

I. Introduction

THE wheelchair is an important aid for the mobility of physically disabled and injured persons, and the push-rim is the preferred mode of propulsion for a large percentage of wheelchair users even though it is associated with the least efficient pattern of propulsion [1]. Extensive research has been performed to understand the biomechanical and physiological factors of wheelchair propulsion [2].

The ergonomics literature indicates that push-rim propulsion (PRP) can lead to severe upper-limb injuries mainly at the shoulder and wrist joints, caused by the discontinuous, highly repetitive and complex upper-limb movements, which reportedly occur during PRP [3]–[5]. Furthermore, high loads at joint excursions exceeding 20°-45° from the neutral position should be avoided for shoulder movements, and even lower joint excursions (18°-30° from the neutral position) are reported to be detrimental at the wrist [6]. Limited information is available on joint angle ranges and joint loads during conventional PRP. Veeger *et al.* [7] measured a mean propulsion force of 30.0N ± 7.1N and a peak propulsion force of 69.4N ± 26.1 N for 20W constant PRP at 1.39m/s linear velocity on a wheelchair dynamometer. Koontz *et al.* [8] simulated wheelchair propulsion over a level, smooth floor at two different speeds – 0.9m/s and 1.8m/s – and reported mean resultant peak propulsion forces of 58.9N ± 11.6N at 0.9m/s and 94.3N ± 26.4N at 1.8m/s. Large variations in upper-limb joint torques are also reported for PRP. Koontz *et al.* [9] analysed kinetics in 27 paraplegic subjects during PRP propulsion on a tile surface at a speed of 0.9m/s and found a peak shoulder abduction/adduction torque of 21.3Nm and shoulder rotation peak torques of 21.6Nm. Collinger *et al.* [10] and Gil-Agudo *et al.* [11] performed measurements under similar conditions and reported peak torques of 7.1Nm/15.3Nm (Collinger *et al.*/Gil-Agudo *et al.*) and 5.8Nm/3.5Nm for shoulder ab-/adduction and shoulder rotation, respectively. Different methods used in these studies to compute joint torques may have contributed to the large variations in the kinetic results. Koontz *et al.* [9] applied a local coordinate system approach whereas Collinger *et al.* [10] and Gil-Agudo *et al.* [11] used custom inverse dynamics models. In addition, PRP patterns are characterized by large variations between subjects and the results are altered by propulsion cadence [12].

Upper-extremity pain and injury represent a major problem for wheelchair dependent persons as use of the arms is essential for independent mobility and participation in the community. Alternative modes for wheelchair propulsion, such as lever-propelled, hub-crank and arm-crank devices, use a continuous cyclic movement for propulsion, which offers higher efficiency compared to conventional PRP [1], [4].

Manuscript received March 25, 2021; revised July 14, 2021; accepted August 11, 2021. Date of publication August 17, 2021; date of current version August 27, 2021. This work was supported by Austrian Science Fund (FWF) under Grant P 25507-B24. *(Corresponding author: Markus Puchinger.)*

This work involved human subjects or animals in its research. Approval of all ethical and experimental procedures and protocols was granted by the Ethikkommission für das Land Niederösterreich under Approval No. GS1-EK-3/149-2018, December 17, 2018.

Markus Puchinger, Pia Stefanek, and Margit Gföhler are with the Research Division of Biomechanics and Rehabilitation Engineering, Department of Engineering Design and Product Development, Technischen Universität Wien (TU Wien), 1060 Vienna, Austria (e-mail: markus.puchinger@tuwien.ac.at).

Karin Gstaltner is with the AUVA Rehabilitation Centre Meidling, 1120 Vienna, Austria.

Marcus G. Pandy is with the Department of Mechanical Engineering, University of Melbourne, Parkville, VIC 3010, Australia.

Digital Object Identifier 10.1109/TNSRE.2021.3105388

The straightforward upper-arm movement during lever-propulsion involves a much larger muscle mass, offers longer push phases and leads to lower strain compared to PRP [13]. Disadvantages are limited top speed of propulsion related to the frequency of the push and recovery phases combined with the absence of pausing between the pushing and pulling phases [13], [14]. The hub-crank mechanism uses cranks that are directly mounted on the hubs of the rear wheels and so allow a continuous motion of the hands. Gross mechanical efficiency (GME) is higher than in PRP, but the position of the hands combined with difficulties in steering and braking make this device impractical [1]. Arm-cranking devices use a continuous cyclic motion for propulsion [1], [4]. The most familiar example of arm-cranking devices is the hand bike, which is a tricycle with the front wheel driven by hand cranks. Handcycling devices are bulky and used mainly outdoors, making them unsuitable for daily living [15], [16]. However, the propulsion form is quite efficient, as propulsion forces are continuously applied over the full cycle, thus resulting in higher efficiency and lower peak forces at the hand and lower loads transmitted to the joints compared to lever propulsion and PRP methods [4], [5], [17].

Arnet *et al.* [5] compared propulsion forces and net shoulder torques during handcycling and PRP at different inclines. The results showed significantly lower mean and peak propulsion forces and lower peak net shoulder torques during handcycling at all inclines.

A major drawback of all currently available alternative propulsion systems is that they can hinder activities of daily living (ADL), as they are usually bulky, heavy and less manoeuvrable. This can be problematic for essential daily activities, such as transfers, backwheel balancing (wheelies) to overcome steps (kerbs), moving the chair over a variety of surfaces or sitting at a table [1], [15]–[18].

To overcome the limitations of PRP, we applied a similar optimization approach to the one described by Rasmussen *et al.* [19] for pedalling. We developed a novel handle-based wheelchair propulsion (HP) device with an ergonomically optimized propulsion shape that offers a continuous cyclic motion at ergonomic joint ranges and is suitable for ADL [20]. The mechanism does not affect the physical width of the wheelchair and was proven to decrease joint excursions and maximum joint torques developed at the wrist [21].

The aim of the present study was to determine the mean and peak propulsion forces, upper-limb joint excursions and net joint torques generated by this novel HP device on an instrumented wheelchair-based test rig. Measurement results from paraplegic subjects propelling the HP device at different loads were compared with PRP data available in the literature. The measurements focussed mainly on the kinematics and kinetics of the shoulder and wrist joints because these are the joints most often affected by propulsion-related injuries [5]. We hypothesized that under similar conditions, HP joint excursions will remain within their ergonomic range and that the effectiveness of the propulsion forces will be higher, leading to lower average propulsion forces compared to PRP. Furthermore, we expected to find lower peak propulsion forces for the HP device due to force application over the full cycle. Based on our previous results [21], we also expected lower net shoulder and wrist torques during HP.

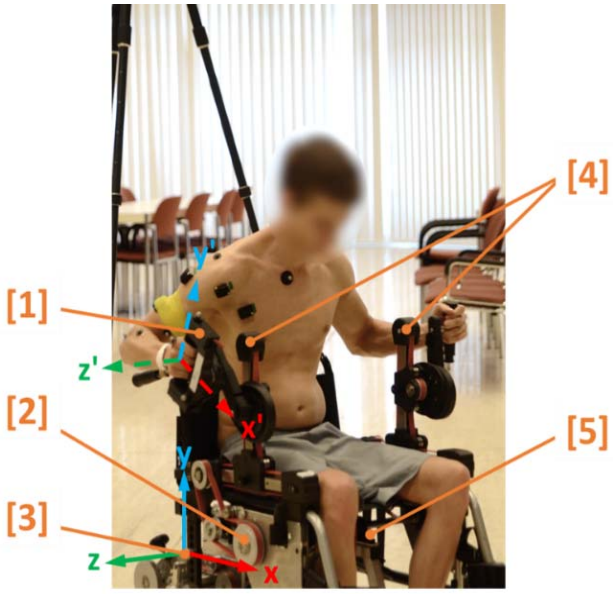

Fig. 1. Wheelchair based test rig. Subject sitting in the wheelchair-based test rig with attached HP devices. [1] handle with integrated force/torque sensor and local coordinate system, [2] resistance power transmission from motor-gear unit to HP devices, [3] global (fixed) coordinate system, [4] HP devices, [5] motor-gear unit.

II. Methods

A. Experimental Setup

All experiments were performed on a wheelchair-based test rig that operated in constant power mode [22] (Fig. 1). Two HP devices [21], [23] were mounted on the test rig instead of the armrests (Fig. 2). Each HP device consisted of a rotating crank on which a handle was mounted. During propulsion, a sliding guide changed the length of the crank over the rotation, and the handle followed the optimized propulsion path.

In accordance with Kurup *et al.* [21] the horizontal position of the crank centre was set to the midpoint between the backrest of the wheelchair and the knee joint position of the subject. For the vertical position, the centre of the crank was set to the height of the elbow joint for upper arm vertically pointing down when seated.

Similar to other studies [24], [25], the test rig was set to simulate linear velocity of 1.1m/s, which simulated the average wheelchair speed used in daily life. The gear ratio of the HP device was fixed at 1.2 for the duration of the experiment, which resulted in an average cadence of ∼50 rpm. This cadence has been found suitable for submaximal handcycling [25].

A custom wireless force-measuring handle with an integrated 3-axis force/torque sensor (K6D40, ME Messsysteme GmbH, Germany) was used to measure propulsion forces and torques. The device was connected to the test rig and the measured data were recorded using Bluetooth. An 8 camera video motion capture system (Kestrel 2200/Cortex 7, Motion

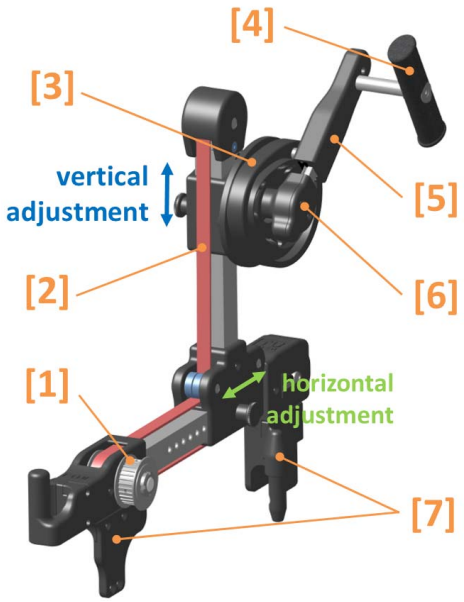

Fig. 2. Handle based propulsion (HP) device and its components. Horizontal and vertical position of the crank centre can be adjusted to the users body measures; [1] timing belt pulley (to the back wheel), [2] timing belt, [3] curve disc, [4] handle, [5] variating crank, [6] crank centre, [7] brackets (fit in armrest mounting).

TABLE I
CHARACTERISTICS OF THE 8 SUBJECTS WITH SPINAL CORD INJURY

Subject (Sex)	Age [yrs]	Weight [kg]	Height [cm]	BMI [kg/m²]	SCI Level
1 (f)	54	62	179	19	T11-12
2 (m)	27	80	188	23	T6-7
3 (f)	43	75	160	29	T10-L1
4 (f)	56	63	158	25	T12-L1
5 (m)	52	65	175	21	T12-L2
6 (m)	45	85	192	23	T11-L1
7 (m)	21	62	185	18	T8-9
8 (m)	51	93	173	31	T12-L2
mean ±SD	44 ±12	73 ±11	176 ±12	24 ±5	

SD: standard deviation; SCI: spinal cord injury

Analysis Corporation, USA) was used to record upper-limb kinematics from each participant.

B. Subjects

Eight right-handed individuals with paraplegia and no history of upper-limb injury participated in this study. Subject characteristics are listed in Table I. All subjects provided informed consent and approval for the study was obtained from the responsible federal state ethics committee (GS1-EK-3/149-2018).

C. Testing Protocol and Data Collection

The force measurement handle was installed on the right side of the wheelchair test rig and side-to-side symmetry was

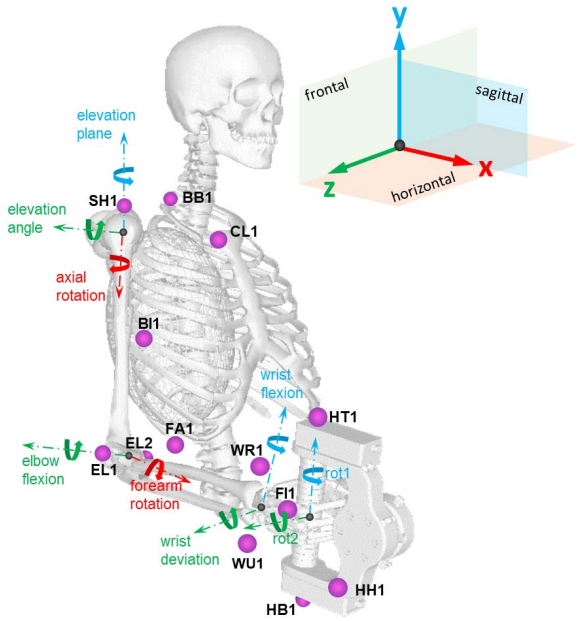

Fig. 3. Biomechanical Model. Upper extremity model with nine degrees of freedom showing the global (fixed) coordinate system and virtual marker placements. Markers were placed at the following locations: clavicle (CL1), acromion (SH1), 7th cervical vertebrae (BB1), biceps (BI1), lateral epicondyle (EL1) and medial epicondyle (EL2), forearm (FA1), radial styloid (WR1), ulnar styloid (WU1), 2nd metacarpophalangeal (MCP) joint (FI1), handle help (HH1), handle top (HT1) and handle bottom (HB1).

assumed during propulsion. Prior to the experimental trials each participant received instructions regarding the propulsion exercises and was given an opportunity to familiarize themselves with the equipment by propelling the wheelchair for 2 minutes without resistance. All trials were performed at two different workloads of 25W and 35W and the same wheelchair velocity of 1.1m/s. Visual feedback on actual and target speed was provided to each participant during propulsion to ensure that a constant speed was maintained during each trial. Each participant performed 10 propulsion cycles at each workload with a two-minute rest interval between the two trials. Ten reflective markers were placed on the participant's trunk and right upper limb and three additional markers were placed on the handle (Fig. 3). Cycles were recorded only after reaching steady propulsion at the target speed, and acceleration and deceleration phases were not included.

D. Biomechanical Model

The upper-extremity model used in this study is based on the *Wheelchair Propulsion (WCP) Model* [26], [27] available in OpenSim [28] and was modified by adding two rotational degrees-of-freedom (DoF) (rot1, rot2) to simulate handle movement. The model comprised of seven rigid bodies (spine and rib cage, clavicle, scapula, humerus, ulna, radius and hand) whose positions and orientations were described by nine degrees of freedom (DoF) (Fig. 3). The kinematic convention recommended by the International Society of Biomechanics

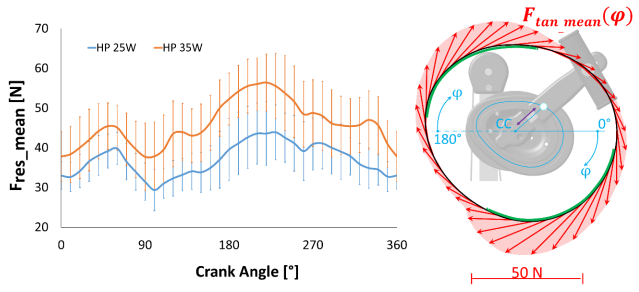

Fig. 4. HP resultant and tangential forces. Left panel: Mean resultant force (F_{res_mean}) and standard deviation for all subjects applied at 25W and 35W. Right panel: Mean tangential forces for all subjects applied at 25W constant resistance with 1.1m/s linear velocity and 50Hz cadence. (CC. . . crank centre, φ. . . crank angle, green highlighted zone $F_{tan} > 30$N).

(ISB) [29]–[31] was used to describe the three rotations at the shoulder (elevation-angle, elevation-plane, axial rotation), elbow flexion, forearm rotation and wrist deviation and flexion. Due to the installed HP devices on both sides and the resulting simultaneous movements of both arms, we expected minor thorax rotations around the x- and y-axes. Rotations of the thorax about the x and y axes were neglected in the model because they were less than ±3° during experiment, whereas thorax rotations around the z-axis were included because they reached ±10° at the higher workload.

For calculation of joint angles and torques, OpenSim 3.3 was used [28]. The simulation process involved the use of three tools available in OpenSim: Scaling, Inverse Kinematics and Inverse Dynamics. First, the model was scaled to each participant's anthropometry based on the measured marker positions when the angular position of the crank was 135°. The scaled model was then used to perform Inverse Kinematics to determine the generalized coordinates (joint angles) at each time step of the motion. Finally, Inverse Dynamics was performed using the reaction forces measured at the handle to compute the generalized net joint torques.

E. Data Analysis

Three-dimensional propulsion forces were measured at the handle bearing using the instrumented handle (Fig. 1). All forces were expressed in the global reference frame of the test rig. The resultant propulsion force ($\hat{F}_{res}$) was calculated as the vector norm of the three measured global force components (F_x, F_y, F_z) during propulsion. For each participant, three cycles with the highest values of F_{res} were used to compute the mean and standard deviation of the resultant force (F_{res_mean}). The average resultant peak force ($\hat{F}_{res\_avg}$) was defined as the average of the highest peak values of F_{res} in all participants across the three cycles. Forces tangential to the handle path (F_{tan}) were calculated with respect to the crank angle (Fig. 4). Mean tangential forces (F_{tan_mean}) with standard deviations were calculated from the same three cycles used to compute F_{res_mean}. The computed net joint torques T_{i,n_0} were normalized by dividing by body weight times body height [32], [33], thus:

$$T_{i,n} = \frac{T_{i,n\_0}}{m_n \cdot g \cdot h_n}$$
$$i = 1 \ldots 10 \text{ generalized coordinate index},$$
$$n = 1 \ldots 8 \text{ participant index} \quad (1)$$

where $T_{i,n}$ is the dimensionless net joint torque, m_n is the participant's body mass in kg, g is the gravitational constant (9.81 m/s^2), and h_n is the participant's body height in meters. The average of the dimensionless normalized joint torque ($T_{i,n}$) or each generalized coordinate calculated across all participants was defined as the averaged normalized joint torque (T_{i_avg}).

Peak torque values for every generalized coordinate and participant ($\hat{T}_{i,n}$) were obtained by averaging the ten highest absolute net torque values (T_{i,n_0}) for the three cycles analyzed. The average peak torque ($\hat{T}_{i\_avg}$) was defined as the average across all participants' peak torques ($\hat{T}_{i,n}$) for each generalized coordinate.

Shoulder joint angles and torques were also expressed in an anatomical meaningful way. Shoulder flexion/extension was defined between the global y-axis (Fig. 3) and the projection of the upper arm onto the sagittal plane whereas shoulder abduction/adduction occurred between the global y-axis and the projection of the upper arm onto the frontal plane. Shoulder horizontal flexion/extension was equivalent to shoulder elevation-plane movement and shoulder internal/external rotation was equivalent to the axial rotation of the shoulder joint. Sagittal flexion, horizontal flexion, abduction, and internal rotation angles were defined as positive. All angles were determined with reference to a neutral anatomic position; that is, with the arm positioned alongside the body and the palm facing medially.

III. Results

A. Handle-Based Propulsion Force

Seven out of the eight participants completed all the trials. One female participant was excluded due to problems with balance during testing. The average of F_{res_mean} across all subjects with respect to a full cycle was 36.9N ± 4.1N (mean ± SD) for 25W and 45.8N ± 5.7N for 35W (Fig. 4, left panel). The average of the applied tangential forces F_{tan_mean} across all participants over a complete cycle was 24.4N ± 5.4N at 25W and 30.6N ± 6.7N at 35W. The participants' individual peak values (>30N) of F_{tan} were applied at crank angle intervals from 10° to 110° and from 190° to 280° for both workloads (Fig. 4, right panel, green highlighted zone). The average resultant peak force ($\hat{F}_{res\_avg}$) was 55.7N ± 11.6N at 25W and 65.4N ± 7.6N at 35W.

B. Joint Kinematics

For both workloads, the range of motion, maximum joint angles and time histories of the joint angles of the shoulder and elbow were almost identical over the full propulsion cycle (Fig. 5 and Table III). The maximum shoulder elevation-plane angle (15.7°/16.0° at 25W/35W) occurred when the handle

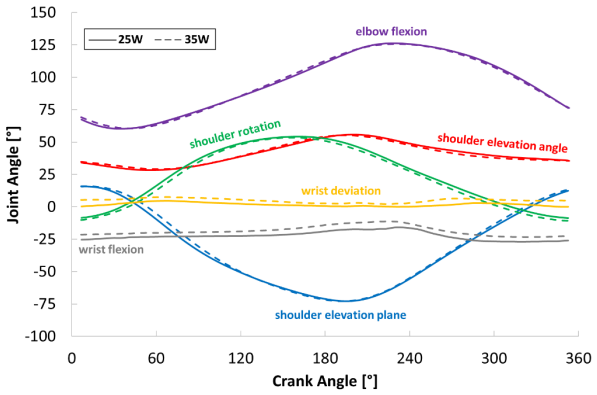

Fig. 5. HP upper-limb joint angles vs. crank angle. Trajectories of the mean upper-limb joint angles averaged across all subjects and all selected cycles over one full crank angle rotation and both workloads. Results shown for HP with resistance levels of 25W (solid lines) and 35W (dashed lines).

was in the foremost position at crank angles between 0° and 10°. The minimum elevation-plane angle (-73.0°/-72.9° at 25W/35W) occurred at the handle's rearmost position at crank angles between 180° to 200°. Peak angles of shoulder elevation (55.8°/55.1° at 25W/35W) occurred at a crank angle of approximately 190°, where the handle was exactly in the rearmost position. The lowest angles of shoulder elevation (28.1°/29.0° at 25W/35W) occurred near the bottom handle position at a crank angle of approximately 80°. Maximum internal rotation was observed shortly before reaching the rearmost position of the handle (135° - 170°). Peak values of external rotation occurred from −10° to 10°, where the handle moved around its foremost position. Elbow flexion increased continually from its lowest value (60.1°/60.6° at 25W/35W) at 45° crank angle to its peak value (126.1°/125.6° at 25W/35W) at 230°, and then decreased in a similar fashion. At the wrist joint, the time histories of joint angles were again identical for both workloads, but the higher load at 35W led to a larger ulnar deviation and a slightly reduced wrist extension over the whole crank rotation. Peak values for ulnar deviation (4.6°/7.5° at 25W/35W) occurred when the crank reached its highest and lowest positions (270° and 70°, respectively) while minimum angles of ulnar deviation (0.0°/2.0° at 25W/35W) occurred at crank angles of 230° and 350°. Peak values of wrist extension (27.0°/23.4° at 25W/35W) occurred at a crank angle of 320° while minimum wrist extension (15.8°/10.9° at 25W/35W) was reached at a crank angle of 230°. When the handle reached its foremost position (crank angle of 0°), the shoulder was maximally flexed in the horizontal direction, outwardly rotated, and elevated to about 35°. The wrist was extended and slightly deviated in the ulnar direction. With increasing crank angle, the shoulder became more horizontally extended, elevated, and rotated inwardly. Wrist extension was reduced whereas ulnar deviation increased rapidly to its maximum at about 80° crank angle and then decreased more slowly to its rearmost position. At the rearmost position (crank angle of 180°), the shoulder was maximally extended in the horizontal direction, elevated, and inwardly rotated. The wrist was minimally extended and in a deviation position close to neutral. As the crank angle increased further, the shoulder flexed in the horizontal direction, reduced in elevation, and was outwardly rotated. The wrist extended and ulnar deviation increased.

C. Joint Torques

The patterns of shoulder joint torque were similar at both workloads (Fig. 6A-C), with higher torques measured at the higher workload as expected. The highest torques for horizontal flexion/extension occurred shortly before and after the peak extension angle when the handle was at its rearmost position. The shoulder elevation torque reached its peak magnitudes during the pull phase, when the handle passed the lowest position, and in the middle of the push phase when the handle was near its uppermost position. In the foremost position of the handle, where the shoulder elevation angle peaked, the elevation torque was relatively low. For shoulder axial rotation, peak values of joint torque occurred in both the push and pull phases, when the shoulder was internally rotated by approximately 20°. When the shoulder was near its maximum and minimum axial rotation angles, the joint torque was again relatively low.

The shapes of the wrist deviation torque trajectories were similar for both workloads (Fig. 6D-E), but the curve representing HP at 35W appeared to be shifted to higher deviation angles. Peak torques occurred when the handle reached its foremost and rearmost positions, where wrist deviation was almost neutral. Wrist flexion showed a different motion pattern at 25W and 35W, with the wrist less extended at the higher load. Peak torque values occurred in foremost and rearmost crank positions at the lower (25W) propulsion resistance, whereas at the higher resistance of 35W peak wrist torques occurred during the pull and push phases.

IV. Discussion

The aim of this study was to measure hand contact forces and upper-extremity joint excursions and joint torques generated by a novel HP device and to compare the results to literature data reported for PRP. We also investigated movement patterns of the shoulder and wrist joints to determine whether high loads occurred at the extreme positions of the joints. Compared to PRP at similar workloads, we found that joint excursions for HP remained within their ergonomic range and that the effectiveness of the propulsion forces was higher, leading to lower average propulsion forces. Thus, our hypothesis was supported. Whilst the model used in this study was based on the WCP Model in OpenSim, we modified its structure by adding two DoFs for movement of the handle. We also provided upper limb kinematic data and hand propulsion forces from experiments as inputs to the model [26], [27]. We found that the model produced torque and moment patterns that were consistent, similar, and repeatable across strokes, speeds and resistance levels.

The average resultant peak forces ($\hat{F}_{res\_avg}$) measured for HP were significantly lower than those reported by Veeger *et al.* [7] and Koontz *et al.* [8] for PRP at lower

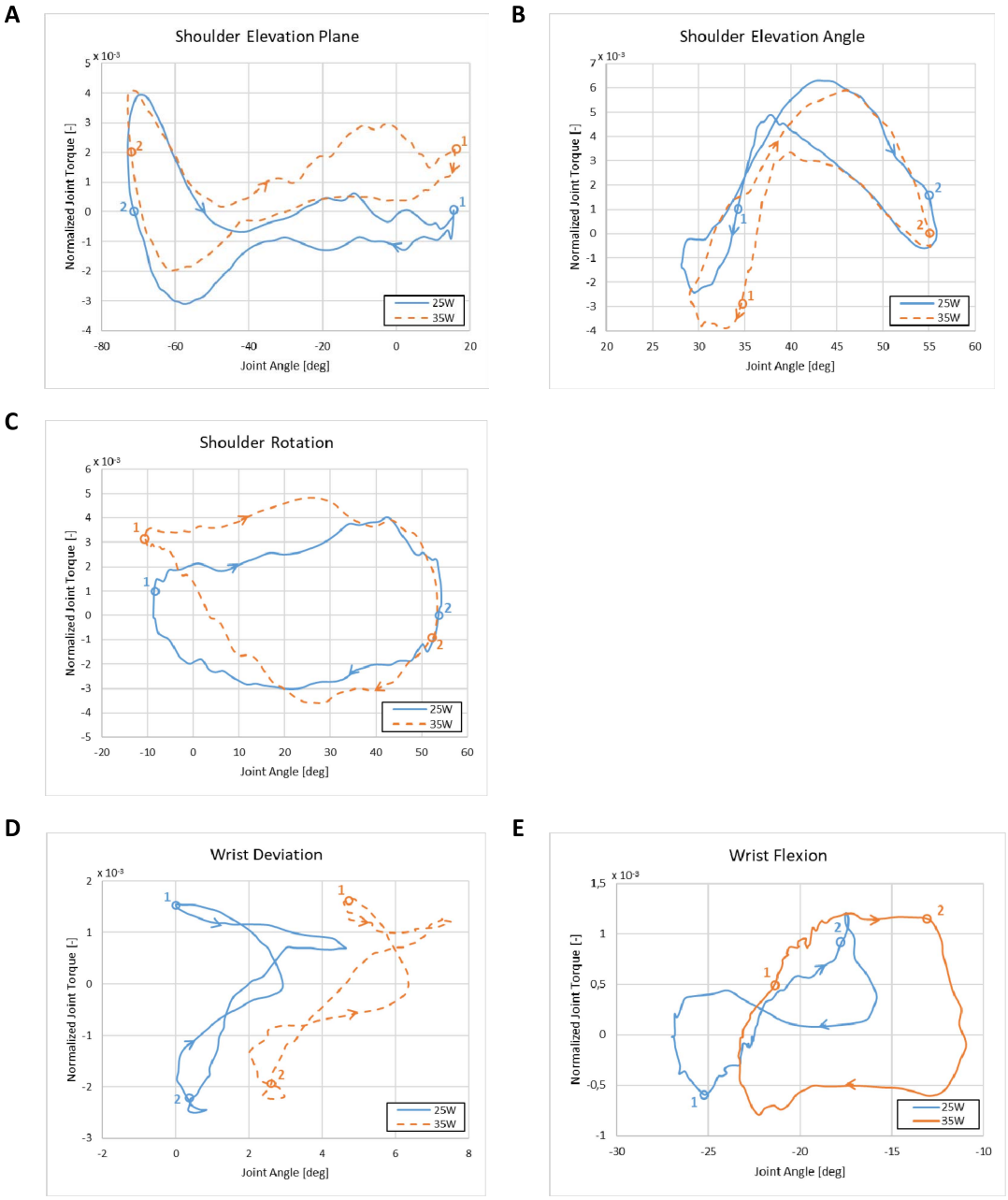

Fig. 6. Joint angles/joint torques. Averaged normalized joint torque-joint angle trajectories generated with HP for: (A) shoulder elevation-plane, (B) shoulder elevation-angle, (C) shoulder rotation, (D) wrist deviation and (E) wrist flexion. The curves illustrate the mean values of all subjects and all selected cycles for each crank angle. HP with resistance levels of 25W (solid blue line) and 35W (dashed orange line) are shown. Position 1 represents a crank angle of 0 degrees while position 2 represents the point when the crank angle reached 180 degrees.

resistance (Table II). Arnet *et al.* [5] performed a similar study and compared joint angle ranges and loads in handcycling with conventional PRP. Their results showed reduced contact forces and continuous force application in handcycling compared to PRP. The reason for this difference between handcycling and PRP relates to the propulsion mode. Propulsion forces can be applied constantly during the whole propulsion cycle in handcycling while in PRP there is always an idle period where no force is applied to the push rim (recovery phase). Similar to the findings of Arnet *et al.* for handcycling, our novel HP device also offers continuous propulsion force application, which results in lower contact forces compared to PRP. Regarding the applied tangential forces with respect to the crank angle, we found that the highest magnitudes were applied shortly after the rearmost and foremost positions of the handle, indicating that our subjects favoured the push and pull phases.

Table III shows comparable results for joint ranges measured during PRP and recommended low impact ergonomic joint excursions. Shoulder elevation-plane movement in HP appears to be slightly shifted to increased horizontal extension and axial rotation to increased external rotation compared to PRP. For both workloads, shoulder abduction and flexion-extension ranges of motion were reduced while maximum

TABLE II
RESULTANT PEAK FORCES DURING HP AND PRP

	Peak	± SD [N]
This study in HP 25W$^{(1.1m/s)}$	**55.7**	**± 11.6**
This study in HP 35W$^{(1.1m/s)}$	**65.4**	**± 7.6**
PRP Koontz 2006 (smooth floor, 0.9m/s)	58.9	± 11.6
PRP Koontz 2006 (smooth floor, 1.89m/s)	94.3	± 26.4
PRP Veeger 2002 (20W, 0.83m/s)	59.3	± 10.7
PRP Veeger 2002 (20W, 1.39m/s)	69.4	± 26.1

Comparison of resultant peak hand propulsion forces ($\hat{F}_{res\_avg}$) in HP and PRP reported in the literature [7, 8]
Test condition is listed in parentheses if multiple conditions were tested

values for abduction were lower than in PRP. Compared to PRP, shoulder extension was lower at both workloads, while shoulder flexion appeared slightly higher at 25W and lower at 35W. Wrist movement changed from a flexion-extension pattern to a full extension movement, and the range of motion was much smaller for HP than for PRP. In comparison to the recommended ergonomic excursions reported in the literature, HP remained within the ergonomic ranges at the wrist, and only for horizontal flexion, abduction and external rotation at the shoulder. Maximum values of the shoulder angles tended to occur at or near a crank angle of 180°, where the handle was near its rearmost position. Highest range of motion values were found in the shoulder elevation-plane and shoulder rotation movement while lower values were observed in the elevation-angle. This finding was consistent for both workloads and explains firstly, that the movement pattern of the arm is guided by the design of the HP, unaffected by the load; and secondly, that the maximum shoulder joint excursions also depend on the subject's seated position relative to the crank centre. All participants were evaluated in the same test wheelchair and no adjustments were made to emulate their current wheelchair setup. Only the horizontal and vertical position of the HP crank centre was modified for each subject to accommodate their body dimensions. If the wheelchair did not fit the subject properly (i.e., the seat was too narrow or too wide, the handle position was too close or too far, or the handle position was too low or too high), this could have resulted in a shifted and inferior shoulder range of motion than would have been the case had the wheelchair fitted the subject optimally. Koontz *et al.* [9], Boninger *et al.* [34] and Rao *et al.* [36] performed a shoulder kinematic analysis for PRP at a lower resistance and a slightly different speed. The comparison of the shoulder joint movements showed no marked differences in horizontal flexion/extension and lower values for both flexion/extension and abduction range of motion. However, shoulder rotation range of motion in HP was about 20° higher and shifted to a more externally rotated position, alternating movement around the neutral position, compared to PRP. This can be explained by the fact that in HP the handle always keeps the hand in front of the subject, in contrast to PRP, where the shoulder is rotated strongly outwards at the beginning of the push phase to ensure an early hand contact with the push rim, and then remains rotated until the end of the push phase [9]. Wrist deviation is very small in HP with a maximum value of 7.5°, whereas large joint angles (12°-23.8°) and range of motion have been reported for PRP. The in literature in HP for wrist flexion was ∼70% lower compared to PRP and ∼80% lower for wrist deviation. Previous studies [34], [35], [37] also report alternating values between wrist flexion-extension and wrist radial-ulnar deviation for PRP, whereas in HP we observed only ulnar deviation close to neutral and wrist extension below 27°.

As shown in Table IV, our average peak shoulder joint torques at 25W are much lower than those reported by Veeger *et al.* [7] and Koontz *et al.* [9] for propulsion at 20W. For both workloads at the wrist, our average peak torque for wrist flexion is below 2Nm and for deviation around 3Nm, which are 7 times lower than the results reported by Boninger *et al.* [34] for similar conditions during PRP. These findings suggest that HP may lead to a reduction in upper-limb injuries compared to PRP [3]–[5]. The normalized torque-crank angle curves at the shoulder joint for both workloads were similar, with only minor propulsion torque differences observed. This effect is seen in Fig. 6, which displays normalized averaged torque values for seven different subjects. There were small differences between subjects in their propulsion patterns, which led to individuals applying peak torques at different joint angles. However, these peaks tended to disappear when the data were averaged across subjects. Average peak torque values as well as peak contact forces values (Table II) of single subjects showed an increase from 25W to 35W. The wrist joint generally showed different torque/angle curves for both resistance levels. Regarding wrist deviation, the propulsion pattern was similar but the range of motion shifted to a more deviated position with increasing workload. This shift can be explained by the fact that at higher resistance forces the subjects tended to grab the handle tighter and hence keep their wrist joints stiffer. Consequently, the range of motion of the wrist moved to a more extended position. Both the propulsion pattern and range of motion for wrist flexion were altered by changing the workload. Because propulsion at 35W increased wrist flexion, higher push and pull forces, which led to a rotation of the wrist during propulsion, were likely caused by the characteristic of the HP drive. Figure 6 shows that the highest joint torques occurred directly after and shortly before the rearmost grip position, where horizontal shoulder extension and internal shoulder rotation also reached their maximum values. As a result, the elbows were directed slightly outwards, forcing the wrist towards extension during propulsion in both the pull and push phases. This fact is also reinforced by the lowest value of flexion in the foremost handle position (Position 2). Conducting further tests at maximum load would likely force subjects into similar propulsion patterns and could strengthen this hypothesis.

TABLE III
MAXIMUM AND MINIMUM JOINT ANGLES IN DEGREES (°) DURING HP AND PRP

	Shoulder elevation-plane [°]			Shoulder elevation-angle [°]			Shoulder flexion [°]			Shoulder abduction [°]			Shoulder rotation [°]			Wrist deviation [°]			Wrist flexion [°]		
	Min	Max	RoM	Min	Max	RoM	Min	Max	RoM	Min	Max	RoM	Min	Max	RoM	Min	Max	RoM	Min	Max	RoM
Normal joint RoM*	-80,0	135,0	215,0	0,0	180,0	180,0	-60,0	170,0	230,0	0,0	180,0	180,0	-70,0	90,0	160,0	-20,0	35,0	55,0	-70,0	80,0	150,0
Ergonomic low impact RoM Keyserling *et al.* 2007	-20,0	45,0	75,0	0,0	45,0	45,0	-20,0	45,0	65,0	0,0	45,0	45,0	-20,0	45,0	75,0	0,0	18,0	18,0	-45,0	30,0	75,0
This Study in HP 25W (1.1m/s)	**-73,0**	**15,7**	**88,7**	**28,1**	**55,8**	**27,7**	**-27,1**	**21,7**	**48,8**	**23,2**	**38,5**	**15,3**	**-8,7**	**54,3**	**63,0**	**0,0**	**4,6**	**4,6**	**-27,0**	**-15,8**	**11,2**
This Study in HP 35W (1.1m/s)	**-72,9**	**16,0**	**88,9**	**29,0**	**55,1**	**26,1**	**-53,9**	**10,7**	**64,6**	**22,9**	**37,0**	**14,1**	**-10,8**	**53,3**	**64,1**	**2,0**	**7,5**	**5,5**	**-23,4**	**-10,9**	**12,4**
Mean of PRP studies	**-58,2**	**26,5**	**88,3**	**22,5**	**56,6**	**34,1**	**-55,4**	**14,9**	**72,1**	**24,3**	**46,3**	**24,1**	**33,1**	**74,6**	**42,5**	**-7,3**	**23,8**	**31,1**	**-30,9**	**17,9**	**48,8**
PRP Koontz *et al.* 2002 (0.9 m/s)	-50,2	34,4	84,6	-	-	-	-43,2	19,1	62,3	26,0	42,0	16,0	24,5	52,1	27,6	-	-	-	-	-	-
PRP Koontz *et al.* 2002 (1,8 m/s)	-52,4	41,2	93,6	-	-	-	-45,4	23,2	68,6	25,0	42,0	17,0	22,8	51,4	28,6	-	-	-	-	-	-
PRP Boninger *et al.* 1998 (1.3 m/s)	-64,9	11,3	86,0	-	-	-	-64,0	6,2	74,8	24,5	47,0	26,1	55,2	90,7	37,3	-	-	-	-	-	-
PRP Boninger *et al.* 1998 (2.2 m/s)	-66,0	22,2	96,9	-	-	-	-68,8	11,1	82,6	21,6	54,2	37,4	51,3	92,8	44,4	-	-	-	-	-	-
PRP Rao *et al.* 1996 (1.5 m/s)	-57,3	23,2	80,5	22,5	56,6	34,1	-	-	-	-	-	-	11,6	86,2	74,6	-7,3	23,8	31,1	-30,9	17,9	48,8
PRP Boninger *et al.* 1997 (1.3 m/s)	-	-	-	-	-	-	-	-	-	-	-	-	-	-	-	-20,0	25,1	41,5	-38,6	7,1	45,7
PRP Boninger *et al.* 1997 (2.2 m/s)	-	-	-	-	-	-	-	-	-	-	-	-	-	-	-	-22,0	21,4	43,4	-34,2	7,4	41,6
PRP Veeger *et al.* 1998 (different inclines & speed)	-	-	-	-	-	-	-	-	-	-	-	-	-	-	-	-24,0	12,0	36,0	-28,0	20,0	48,0
PRP Wei *et al.* 2003 (high middle position)	-	-	-	-	-	-	-	-	-	-	-	-	-	-	-	-26,0	17,0	43,0	-35,0	10,0	45,0

Comparison of maximum and minimum joint angles and range of motion (RoM) at the shoulder and wrist [6, 9, 34–38]
Test condition is listed in parentheses if multiple conditions were tested
*values are according to the American Academy of Surgeons (AAOS)

From an ergonomic standpoint, it is recommended to keep joint angles close to their neutral positions for the duration of the movement [6]. Considering the propulsion pattern and the torque curves for HP, our results indicate that propelling the wheelchair with this novel propulsion device produces a more ergonomic range of motion of the upper-limb joints compared to PRP.

There are limitations of our study that ought to be considered when interpreting the results. First, the crank handle of the test wheelchair was not adjustable in the medial-lateral (z) direction to account for individual differences in body anthropometry, which may have influenced the performance (i.e., kinematics and kinetics) of the HP device. Second, the sample size (n=8) was relatively small. Force application during wheelchair propulsion is highly individualized, particularly for PRP, thus a larger number of test subjects would be required for greater statistical strength. However, the sample size used in the present study was limited by the availability of paraplegic patients who were willing and able to participate in these experiments. Future studies should consider performing maximum power tests at different power levels with a larger group of individuals to obtain a statistically significant inter-subject comparison of HP and PRP.

In this study, we focus on kinematic and kinetic variables during steady propulsion, using the novel wheelchair drive device which has been computationally optimised for maximum power output [20]. Due to the possibility of applying propulsion forces over the entire cycle in combination with the selected gear ratio, we also expect that mobility will be significantly improved in practical use. Especially activities in daily life which require higher drive torques, such as start-up, acceleration, uneven ground or driving on ramps, are much easier to handle with the novel wheelchair propulsion device, which has also been confirmed by first tests. Furthermore, it is possible to propel both in synchronous and asynchronous mode, which can be advantageous for different situations in

TABLE IV
PEAK JOINT TORQUES IN HP AND PRP

	Shoulder elevation-plane	Shoulder elevation-angle	Shoulder rotation	Wrist deviation	Wrist flexion
	Peak ± SD [Nm]	Peak ± SD [Nm]	Peak ± SD [Nm]	Peak ± SD [Nm]	Peak ± SD [Nm]
This study in HP 25W	**5.2 ± 2.1**	**7.2 ± 3.2**	**5.2 ± 2.8**	**2.8 ± 1.5**	**1.5 ± 0.9**
This study in HP 35W	**5.5 ± 2.0**	**7.9 ± 3.3**	**6.1 ± 3.3**	**3.1 ± 1.6**	**1.6 ± 0.6**
PRP Koontz *et al.* 2002 (9.24W, 0.9m/s)	10.9 ± 6.3	21.3 ± 12.0	21.6 ± 5.9	-	-
PRP Koontz *et al.* 2002 (21.85W, 1.3m/s)	21.0 ± 10.2	31.1 ± 14.1	31.9 ± 10.7	-	-
PRP Veeger *et al.* 2002 (20W, 0.83m/s)	21.7 ± 3.7	12.1 ± 4.9	9.8 ± 1.4	-	-
PRP Veeger *et al.* 2002 (20W, 1.39m/s)	21.1 ± 0.9	16.0 ± 8.6	11.7 ± 3.1	-	-
PRP Boninger et al. 1997 (14W, 1.3m/s)	-	-	-	16.6 ± 8.8	10.4 ± 4.8
PRP Boninger *et al.* 1997 (23W, 2.2m/s)	-	-	-	21.3 ± 11.7	13.6 ± 5.1

Average peak torques during HP calculated for 25W and 35W workloads and compared to peak torque values for PRP reported in the literature [7, 9, 35].
Test condition is listed in parentheses if multiple conditions were tested

everyday life. With the brakes integrated for everyday use, the wheelchair can be decelerated in controlled fashion whereas for certain situations, such as overcoming steps, the push-rims on the wheelchair wheels can still be used. Future HP devices should offer a reverse gear and the possibility to lower the cranks, which is most important for transfers or driving under tables. However, we see our HP device as more suitable for indoor use, but it can also be used in an urban environment.

V. CONCLUSION

Overall, we found that our novel HP device improved wrist motion during wheelchair propulsion. In addition, shoulder rotation motion was optimized while shoulder elevation-plane motion remained relatively unchanged compared to PRP. However, our results indicate that HP is associated with reduced joint torques and lower joint excursions compared to PRP. Future work should focus on optimizing handle positions and determining whether improved joint ranges of motion may be achieved, especially for the shoulder elevation-plane, by increasing the distance between the crank centre and the body.

REFERENCES

[1] L. H. V. van der Woude, A. J. Dallmeijer, T. W. J. Janssen, and D. Veeger, "Alternative modes of manual wheelchair ambulation: An overview," *Amer. J. Phys. Med. Rehabil.*, vol. 80, no. 10, pp. 765–777, Oct. 2001, doi: 10.1097/00002060-200110000-00012.

[2] L. van der Woude, H. Veeger, A. Dallmeijer, T. Janssen, and L. Rozendaal, "Biomechanics and physiology in active manual wheelchair propulsion," *Med. Eng. Phys.*, vol. 23, no. 10, pp. 713–733, 2001, doi: 10.1016/S1350-4533(01)00083-2.

[3] J. L. Mercer, M. Boninger, A. Koontz, D. Ren, T. Dyson-Hudson, and R. Cooper, "Shoulder joint kinetics and pathology in manual wheelchair users," *Clin. Biomech.*, vol. 21, no. 8, pp. 781–789, Oct. 2006, doi: 10.1016/j.clinbiomech.2006.04.010.

[4] U. Arnet, S. Drongelen, A. Scheel-Sailer, L. Woude, and D. Veeger, "Shoulder load during synchronous handcycling and handrim wheelchair propulsion in persons with paraplegia," *J. Rehabil. Med.*, vol. 44, no. 3, pp. 222–228, 2012, doi: 10.2340/16501977-0929.

[5] U. Arnet, S. van Drongelen, D. Veeger, and L. H. V. van der Woude, "Force application during handcycling and handrim wheelchair propulsion: An initial comparison," *J. Appl. Biomech.*, vol. 29, no. 6, pp. 687–695, Dec. 2013, doi: 10.1123/jab.29.6.687.

[6] W. M. Keyserling, D. S. Stetson, B. A. Silverstein, and M. L. Brouwer, "A checklist for evaluating ergonomic risk factors associated with upper extremity cumulative trauma disorders," *Ergonomics*, vol. 36, no. 7, pp. 807–831, Jul. 1993, doi: 10.1080/00140139308967945.

[7] H. Veeger, L. A. Rozendaal, and F. van der Helm, "Load on the shoulder in low intensity wheelchair propulsion," *Clin. Biomech.*, vol. 17, no. 3, pp. 211–218, 2002, doi: 10.1016/S0268-0033(02)00008-6.

[8] A. M. Koontz *et al.*, "Investigation of the performance of an ergonomic handrim as a pain-relieving intervention for manual wheelchair users," *Assistive Technol.*, vol. 18, no. 2, pp. 123–145, Sep. 2006, doi: 10.1080/10400435.2006.10131912.

[9] A. M. Koontz, R. A. Cooper, M. L. Boninger, A. L. Souza, and B. T. Fay, "Shoulder kinematics and kinetics during two speeds of wheelchair propulsion," *J. Rehabil. Res. Develop.*, vol. 39, no. 6, pp. 635–649, 2002.

[10] J. L. Collinger *et al.*, "Shoulder biomechanics during the push phase of wheelchair propulsion: A multisite study of persons with paraplegia," *Arch. Phys. Med. Rehabil.*, vol. 89, no. 4, pp. 667–676, Apr. 2008, doi: 10.1016/j.apmr.2007.09.052.

[11] A. Gil-Agudo, A. D. Ama-Espinosa, E. Pérez-Rizo, S. Pérez-Nombela, and B. Crespo-Ruiz, "Shoulder joint kinetics during wheelchair propulsion on a treadmill at two different speeds in spinal cord injury patients," *Spinal Cord*, vol. 48, no. 4, pp. 290–296, Apr. 2010, doi: 10.1038/sc.2009.126.

[12] M. L. Boninger, A. L. Souza, R. A. Cooper, S. G. Fitzgerald, A. M. Koontz, and B. T. Fay, "Propulsion patterns and pushrim biomechanics in manual wheelchair propulsion," *Arch. Phys. Med. Rehabil.*, vol. 83, no. 5, pp. 718–723, May 2002, doi: 10.1053/apmr.2002.32455.

[13] C. McLaurin and C. Brubaker, "Lever drive system for wheelchairs," *J. Rehabil. Res. Develop.*, vol. 23, pp. 52–54, Apr. 1986.

[14] A. R. Sarraj and R. Massarelli, "Design history and advantages of a new lever-propelled wheelchair prototype," *Int. J. Adv. Robotic Syst.*, vol. 8, no. 3, p. 26, Aug. 2011, doi: 10.5772/10669.

[15] P. A. Smith, R. M. Glaser, J. S. Petrofsky, P. D. Underwood, G. B. Smith, and J. J. Richard, "Arm crank vs handrim wheelchair propulsion: Metabolic and cardiopulmonary responses," *Arch. Phys. Med. Rehabil.*, vol. 64, no. 6, pp. 249–254, 1983.

[16] G. Mukherjee and A. Samanta, "Physiological response to the ambulatory performance of hand-rim and arm-crank propulsion systems," *J. Rehabil. Res. Develop.*, vol. 38, no. 4, pp. 391–399, 2001.

[17] U. Arnet, S. van Drongelen, L. H. V. van der Woude, and D. H. E. J. Veeger, "Shoulder load during handcycling at different incline and speed conditions," *Clin. Biomech.*, vol. 27, no. 1, pp. 1–6, Jan. 2012, doi: 10.1016/j.clinbiomech.2011.07.002.

[18] C. L. Flemmer and R. C. Flemmer, "A review of manual wheelchairs," *Disab. Rehabil., Assistive Technol.*, vol. 11, no. 3, pp. 177–187, Apr. 2016, doi: 10.3109/17483107.2015.1099747.

[19] J. Rasmussen, S. T. Christensen, M. Gföhler, M. Damsgaard, and T. Angeli, "Design optimization of a pedaling mechanism for paraplegics," *Struct. Multidisciplinary Optim.*, vol. 26, nos. 1–2, pp. 132–138, Jan. 2004, doi: 10.1007/s00158-003-0324-5.

[20] N. Babu Rajendra Kurup, M. Puchinger, and M. Gföhler, "Forward dynamic optimization of handle path and muscle activity for handle based isokinetic wheelchair propulsion: A simulation study," *Comput. Methods Biomech. Biomed. Eng.*, vol. 22, no. 1, pp. 55–63, Jan. 2019, doi: 10.1080/10255842.2018.1527321.

[21] N. B. R. Kurup, M. Puchinger, T. Keck, and M. Gfoehler, "Wrist kinematics and kinetics during wheelchair propulsion with a novel handle-based propulsion mechanism," in *Proc. 40th Annu. Int. Conf. IEEE Eng. Med. Biol. Soc. (EMBC)*, Jul. 2018, pp. 2146–2149, doi: 10.1109/EMBC.2018.8512658.

[22] M. Puchinger, N. B. R. Kurup, and M. Gföhler, "A test rig for investigating manual wheelchair propulsion devices—TAR 2017–March 09–10," *Current Directions Biomed. Eng.*, vol. 3, p. 12, Mar. 2017, doi: 10.1515/cdbme-2017-1001.

[23] N. B. R. Kurup, M. Puchinger, and M. Gfoehler, "A preliminary muscle activity analysis: Handle based and push-rim wheelchair propulsion," *J. Biomech.*, vol. 89, pp. 119–122, May 2019, doi: 10.1016/j.jbiomech.2019.04.011.

[24] M. L. Boninger, R. A. Cooper, R. N. Robertson, and S. D. Shimada, "Three-dimensional pushrim forces during two speeds of wheelchair propulsion," *Amer. J. Phys. Med. Rehabil.*, vol. 76, no. 5, pp. 420–426, Sep. 1997, doi: 10.1097/00002060-199709000-00013.

[25] A. J. Dallmeijer, L. Ottjes, E. de Waardt, and L. H. V. van der Woude, "A physiological comparison of synchronous and asynchronous hand cycling," *Int. J. Sports Med.*, vol. 25, no. 8, pp. 622–626, Jul. 2004, doi: 10.1055/s-2004-817879.

[26] B. Odle, J. Reinbolt, G. Forrest, and T. Dyson-Hudson, "Construction and evaluation of a model for wheelchair propulsion in an individual with tetraplegia," *Med. Biol. Eng. Comput.*, vol. 57, no. 2, pp. 519–532, Feb. 2019, doi: 10.1007/s11517-018-1895-z.

[27] B. Odle, G. Forrest, J. Reinbolt, and T. Dyson-Hudson, "Development of an OpenSim shoulder model for manual wheelchair users with tetraplegia," in *Proc. ASME Int. Mech. Eng. Congr. Expo.*, vol. 2. Denver, CO, USA: ASMEDC, 2011, pp. 541–542, doi: 10.1115/IMECE2011-64816.

[28] S. L. Delp *et al.*, "OpenSim: Open-source software to create and analyze dynamic simulations of movement," *IEEE Trans. Biomed. Eng.*, vol. 54, no. 11, pp. 1940–1950, Nov. 2007, doi: 10.1109/TBME.2007.901024.

[29] G. Wu *et al.*, "ISB recommendation on definitions of joint coordinate systems of various joints for the reporting of human joint motion—Part II: Shoulder, elbow, wrist and hand," *J. Biomech.*, vol. 38, no. 5, pp. 981–992, May 2005, doi: 10.1016/j.jbiomech.2004.05.042.

[30] K. R. Saul *et al.*, "Benchmarking of dynamic simulation predictions in two software platforms using an upper limb musculoskeletal model," *Comput. Methods Biomech. Biomed. Eng.*, vol. 18, no. 13, pp. 1445–1458, Oct. 2015, doi: 10.1080/10255842.2014.916698.

[31] K. R. Saul, S. Hayon, T. L. Smith, C. J. Tuohy, and S. Mannava, "Postural dependence of passive tension in the supraspinatus following rotator cuff repair: A simulation analysis," *Clin. Biomech.*, vol. 26, no. 8, pp. 804–810, Oct. 2011, doi: 10.1016/j.clinbiomech.2011.04.005.

[32] J. W. Wannop, J. T. Worobets, and D. J. Stefanyshyn, "Normalization of ground reaction forces, joint moments, and free moments in human locomotion," *J. Appl. Biomech.*, vol. 28, no. 6, pp. 665–676, Dec. 2012, doi: 10.1123/jab.28.6.665.

[33] M. P. Kadaba, H. K. Ramakrishnan, M. E. Wootten, J. Gainey, G. Gorton, and G. V. Cochran, "Repeatability of kinematic, kinetic, and electromyographic data in normal adult gait," *J. Orthopaedic Res.*, vol. 7, no. 6, pp. 849–860, 1989, doi: 10.1002/jor.1100070611.

[34] M. L. Boninger, R. A. Cooper, S. D. Shimada, and T. E. Rudy, "Shoulder and elbow motion during two speeds of wheelchair propulsion: A description using a local coordinate system," *Spinal Cord*, vol. 36, no. 6, pp. 418–426, Jun. 1998, doi: 10.1038/sj.sc.3100588.

[35] M. L. Boninger, R. A. Cooper, R. N. Robertson, and T. E. Rudy, "Wrist biomechanics during two speeds of wheelchair propulsion: An analysis using a local coordinate system," *Arch. Phys. Med. Rehabil.*, vol. 78, no. 4, pp. 364–372, 1997, doi: 10.1016/S0003-9993(97)90227-6.

[36] S. S. Rao, E. L. Bontrager, J. K. Gronley, C. J. Newsam, and J. Perry, "Three-dimensional kinematics of wheelchair propulsion," *IEEE Trans. Rehabil. Eng.*, vol. 4, no. 3, pp. 152–160, Sep. 1996, doi: 10.1109/86.536770.

[37] H. E. Veeger, L. S. Meershoek, L. H. van der Woude, and J. M. Langenhoff, "Wrist motion in handrim wheelchair propulsion," *J. Rehabil. Res. Develop.*, vol. 35, no. 3, pp. 305–313, 1998.

[38] S. Wei, S.-L. Huang, C.-J. Jiang, and J.-C. Chiu, "Wrist kinematic characterization of wheelchair propulsion in various seating positions: Implication to wrist pain," *Clin. Biomech.*, vol. 18, no. 6, pp. S46–S52, 2003, doi: 10.1016/S0268-0033(03)00084-6.